Osteoblastic Activity and Vascular Development of BMSCs and TCP Constructs *In Vivo* Evaluated by Bone Scintigraphy

Dan Li, Tingliang Wang, Guangdong Zhou and Lian Zhu*

Department of Plastic and Reconstructive Surgery, Shanghai 9th People's Hospital, Jiao Tong University School of Medicine, People's Republic of China

Abstract: Osteogenic and vascular potential in bone regenerative therapy has been mainly examined in an animal-implantation study. We have here evaluated the applicability of bone scintigraphy in imaging bone formation, especially in its initial phase. The defect at the mid-portion of the double ulna in each canine was repaired with β-TCP cylinder alone (control group n=8) or BMSCs and β-TCP cylinder compound (experimental group n=8). Bone formation in the defects was compared between the two groups in the same ways. By radionuclide scintigraphy, significant difference was observed between the two groups at month one and two, but no significant difference at month three. The result showed osteoblastic activity persisted more in the defect repaired with BMSCs and β-TCP cylinder compound than with β-TCP cylinders alone. In conclusion, the bone scintigraphic methodology, although exhibiting less quantitation and resolution, could be applicable as a non-invasive, highly sensitive methodology in detecting the initial, microscopic changes associated with mineralization in tissue-engineered bone.

Keywords: Tissue-engineering, bone formation, porous β-tricalciumphosphat, Radionuclide scintigraphy, nuclear medicine.

INTRODUCTION

Tissue engineering has been shown to be an effective approach in bone regeneration. Many kinds of material combined with bone marrow stem cell (BMSC) have been developed to be appropriated bone graft for different regions of skeleton. Regarding the application of repairing long, weight-bearing bone, synthetic calcium phosphate ceramics such as β-tricalcium phosphate are common used as bone substitutes for its high tissue compatibility and rapid biodegradation, which has been demonstrated to be efficacious in many large mammals, such as sheep and canine [1-4].

Foundation of bone formation, proposed by Albrektsson [5], is the osseointegration between living bone and the implant. Other author confirmed the important of early and stably post-transplantative vascularization of the implant for successful osseointegration [6-9].

Several examinations were classic used to observe the bone-healing process around implants, such as histological examination, X-ray and computed tomography. However, histological examination is not suitable to observe the same site of implant in different periods with noninterference to the healing process, so it is not a suitable technique for observation in clinical practice. X-ray examination is capable of determining the level of mineralization, but with low sensitivity in the detection of early pathologic and/or bone remodelling changes [10]. Computed tomography (CT) based on X-ray has made it possible to evaluate small changes in bone mass and structure, which has a high resolution in μm range and can own high sensitivity in the detection, but it is impossible to display bone surviving before 6 to 8 weeks [11, 12]. Most importantly, X-ray and CT cannot monitor the details of vascularization and osteogenic activity of the implant.

In contrast, bone scintigraphy is known to have a high sensitivity in osteogenic activity and local vascularization, which is based on the evidence that Tc-99m MDP (^{99m}Tc-hydroxymethyl diphosphonate) is accumulated by local blood flow at the site of mineralization in proportion to the level of newly formed calcium phosphate crystals. So Tc-99m MDP is useful for assessment of local tissue blood perfusion and for detecting bone formation or bone infarction in clinical practice [13-15].

In this study, we used bone scintigraphy to evaluate the vascularization and osseointegration of porous β-TCP combined with BMSCs, which was implanted to heal the ulna defect in a canine model as tissue-engineered bone.

MATERIAL AND METHODS

BMSCs Isolation and Culture

After anesthetization through intramuscular injection of 10 mg/kg ketamine, autologous bone marrow (5 mL in total volume) was harvested by iliac aspiration from

*Address correspondence to this author at the Department of Plastic and Reconstructive Surgery, Shanghai 9th People's Hospital, Jiao Tong University School of Medicine, People's Republic of China; Tel: +0086-021-23271699 (ext. 5120); E-mail: zhulian6@hotmail.com

E-ISSN: 2311-9888/14

each adult Canine. The iliac bone marrow was separated by percoll (1.073 g/mL; Sigma, St. Louis, MO) gradient centrifugation and the mononuclear cells were plated in 100mm^2 dishes (Falcon, Franklin Lakes, NJ) at a density of 1×10^5 cells/cm^2. Cells were cultured in osteogenic induction media (Dulbecco's modified Eagle's medium; Gibco, Grand Island, NY) supplemented with 10% heated inactive fetal bovine serum (Gibco), 10^{8}mmol/L dexamethasone, 10 mmol/L β-phosphoglycerol, and 50 mmol/L L-2-ascorbic acids (all from Sigma) at 37^{0}C with 5% CO_2. The culture medium was changed after 48 h and then every 3 days. When BMSCs reached at 80–90% confluence, cells were detached with 0.25% trypsin/ethylenediamin-etetraacetic acid (Gibco) and sub-cultured at a density of 1×10^5 cells/cm$_2$ in 100mm dishes. Cells within three passages were used in the following experiment.

Preparation of Cell- Porous β-TCP

Porous β-TCP were obtained from Mediterranean university in Franc and used as the scaffold. The scaffold was molded into a cylinder 20 mm high, and 8 mm in outer diameter, 5mm in inner diameter (Figure **1**) and a cube of 3×3×3 mm^3.β-TCP implants were sterilized by autoclaving, a process that does not affect the β-TCP composition. Autologous BMSCs cultured *in vitro* were detached from culture dishes by the treatment of trypsin (0.25%) / EDTA (0.01%), after which, they were centrifuged to remove media and then resuspended in the media at a cellular density of 20×10^6/ml. The cell suspension was slowly added to the β-TCP by instillation (approximately 2.5ml per cylinder and 0.4ml per cube). The cell-β-TCP construct was then placed in an incubator for four hours. Subsequently, 30 ml of induced medium were added and the construct was completely submerged into the medium and incubated at 37ºC in 5%CO_2 followed by medium change every two days. The cell-cube hybrids, after incubation for one, three, five and seven days respectively, were consecutively rinsed two times with PBS and then fixed in 2% formalin for two hours. Finally, the cubes were broken into two halves and the broken surface was sprinkled with aurum powder and processed for scanning electron microscopy (SEM XL-30 Philips Holland) examination to evaluate cell adhesion and cell penetration. Cell-cylinder hybrids were co-cultured *in vitro* for a period of seven days prior to surgery and were then implanted to the ulna defect of the respective canines.

Animals Surgical Procedure

The experimental protocol was approved by the Animal Care and Experiment Committee of Shanghai Jiao Tong University School of Medicine. A total of 8 healthy adult canines with an average weight of 17.5kg were included in this study. The animals were anesthetized through intramuscular injection of 20 mg/kg ketamine. The aspect of the right ulna shaft was exposed through a 5 cm longitudinal incision using a standard lateral approach to the ulna. Then an osteoperiosteal segmental cortical defect, 20mm long and representing approximately 20 percent of the ulna's total length, was made at the mid-portion of the diaphysis with an oscillating bone saw that was cooled continuously through saline irrigation. Care was taken to remove all bone debris and spilled marrow particulates. The right ulna defects were filled with β-TCP cylinder plus induced BMSCs (Figure **2**) as experimental group. On the left ulna, the defect was as the same as that on the right side, but filled by the

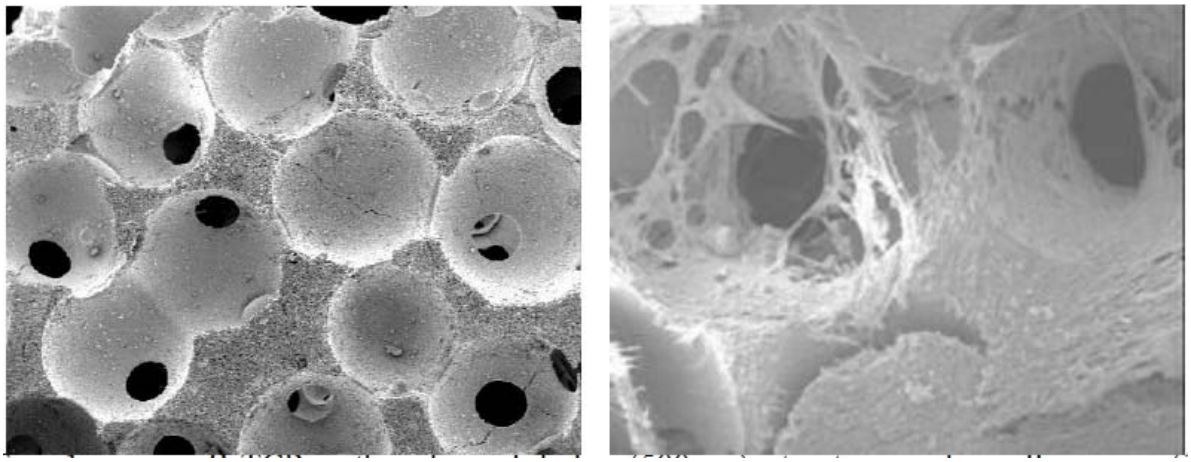

Figure 1: porous β-TCP with spherical holes (500μm) structure and small opening (100μm) as anastomosing network (left) After 7days *in vitro* culture, the cells with an abundant surrounding matrix filled inside the apertures (right).

cylinder alone without cells as the control group. The subcutaneous and skin layers were closed in the routine manner. Postoperatively, each of the animals was given intramuscular penicillin injection for 3 days, twice per day, 800,000 Unit for each time. Each of the animals was housed in a $16m^2$ pen and fed a maintenance ration of hay plus free access to water for the duration of the study.

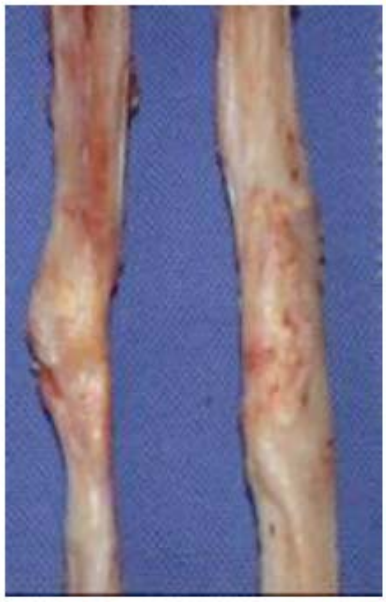

Figure 2: Three months after operation, the diameter of ulnar was still shorter in control group (right). The boundary of new bone and remainder diaphysis of the ulna disappeared in all animals. The new bone in experiment had been with red and white color (left), while the new bone was of infirmity in control group.

Radiographic, Gross Observation and Histological Examination

Postoperatively, after one and three months, radiographs of both sides of the ulars were obtained under general anesthesia. Radiographs were evaluated for evidence of new bone formation within the defect.

Animal were separately sacrificed with an overdose of intravenously administered pentobarbital sodium (one animal at one month after operation, and seven animals at three months after the operation). The soft tissue was stripped from the double ulnar. The defect site of the double ulnar was assessed by gross observation, including osteojuncture, length, color and texture. Transected tissue from the middle portion of the original defect area was fixed with 4% paraformaldehyde for 72h and decalcified with 8% HCl in PBS, 5% formic acid and 7% aluminum chloride in PBS for another 48h. The tissues were then embedded in paraffin and sectioned for hematoxylin and eosin staining.

Bone Scintigraphy

In the three months after operation, bone scintigraphies were taken every month. The canines was anesthetized through intramuscular injection of 20 mg/kg ketamine to be general anesthesia state and were fixed on sample table in prone position, and then 18MBq/kg technetium 99m labelled methylene diphosphonate (99mTcm-MDP) was given by femoral vein. Immediately after injection, dynamic images were continuously acquired for reference, and static images obtained after two hours, radionuclide bone imaging of parallel front legs of animals were obtained with a Sopha media DS7 SPEC. For each delayed image, 256×256 matrix of data was acquired. Radioactive gathered several T(ROI) (region of interest)was drawn around each detected area on the scintigraphic images. Another ROI (NT) was also drawn on the sound part of ulnar. T/NT rates were calculated for each animal. A paired T-test was carried out to find out whether there were significant differences between the left and the right implant sides and the significance level was accepted as $P < 0.05$.

RESULTS

Scanning Electron Microscope Examination

Scanning electron microscope (SEM) examination showed that the microstructure of a porous β-TCP was homogeneously spherical holes (500μm) structure with small opening (100μm) as anastomosing network. After 7days of induced *in vitro* culture, the cells were in abundance and spread flat on the surface like fibroblasts within an abundant surrounding matrix filled inside the apertures that were interconnected to each other (Figure **1**). Accordingly, in this study, day 7 was an appropriate time point to implant the constructs *in vivo*.

Gross Observation

All animals survived the surgical procedure with no infection at the site of implantation. They were able to move normally at the third day after operation. As to the one animal sacrificed at one month after operation, the diameter of ulnar was shorter in left than in right. The implant in left was difficult to detach for the fibroid tissue around it, but in right. There was much more new bone with larger volume, and the surface was rough. As to the six animals sacrificed at three months

after operation, the diameter of ulnar was still shorter in control group than in experimental group as before, but the boundary of new bone and remainder diaphysis of the ulna disappeared in all animals. The new bone in experiment had been obviously remodeled with red and white color, while the new bone was of infirmity in volume and form in control group (Figure **2**).

Radiographic Analyses

No significant difference between the two ulnar immediately after operation was observed by X-ray after surgery (Figure **3-a**). At one month after operation, the defect was better bridged by the implant with obscure edge in experimental group, new bone formed at the canal and the interface, but in control group, the implant was obviously deformed into dissociated granule with non-uniform density, especially at the middle portion, but some new bone formed at the interface (Figure **3-b**). At three months after operation, the defect was bridged by new bone with osteodermatous cavum medullare ossium in experiment group, while in the control group, the defect was bridged by high density material without osteodermatous cavum medullare ossium, the diameter of the ular was obviously less than another one (Figure **3-c**).

Histological Examination

Hematoxylin and Eosin (HE) staining of three months in experimental group demonstrated that β-

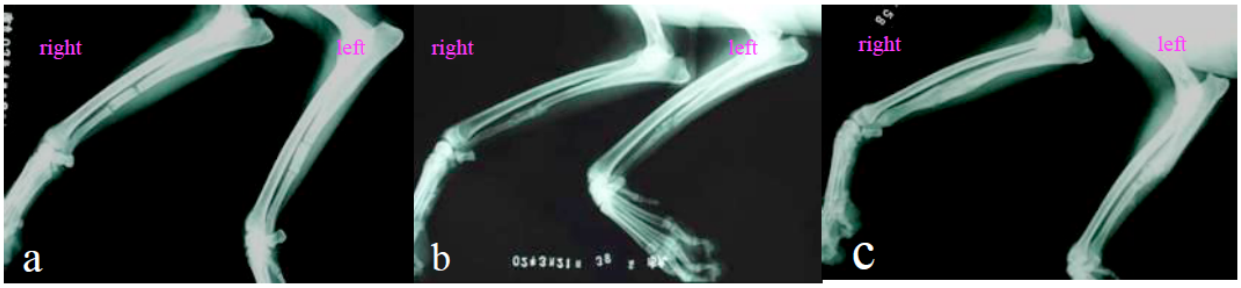

Figure 3: No significant difference between the two ulnar immediately after operation (**a**). At one month, new bone formed at the canal and the interface in experimental group, while in control group, the implant was obviously deformed into dissociated granule, especially at the middle portion, some new bone formed at the interface (**b**). At three months, the defect was bridged by new bone with osteodermatous cavum medullare ossium in experiment group, while in the control group, the defect was bridged by high density material without osteodermatous cavum medullare ossium (**c**).

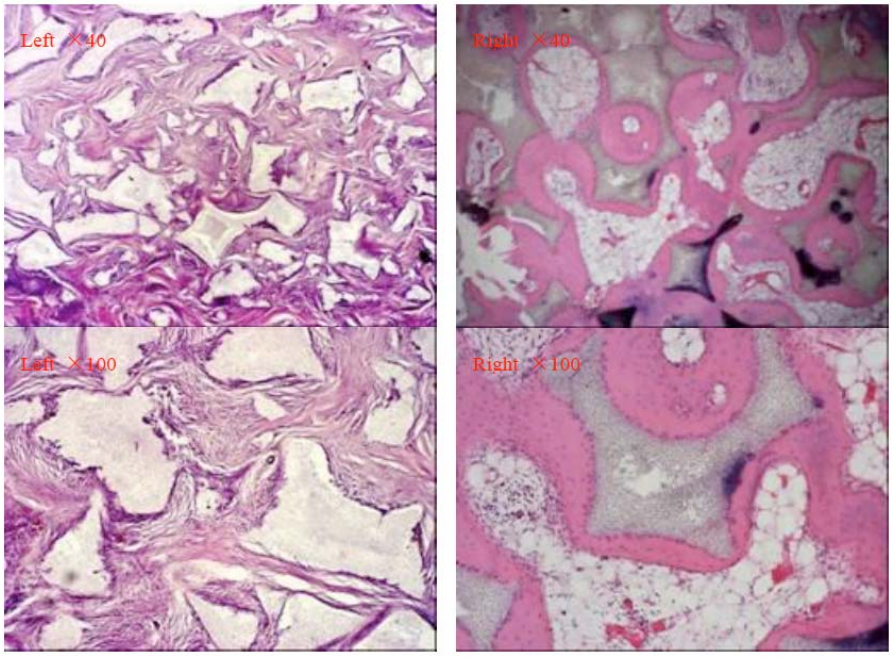

Figure 4: HE at three months, β-TCP degraded into fine granule and new bone adhered to the surface on the core of β-TCP in experimental group (right). While in control group, the degradation percentage was more than that of experimental group, osteoblasts arranged on the surface of β-TCP holes, and osteoid was observed with much megacayocytes at the core.

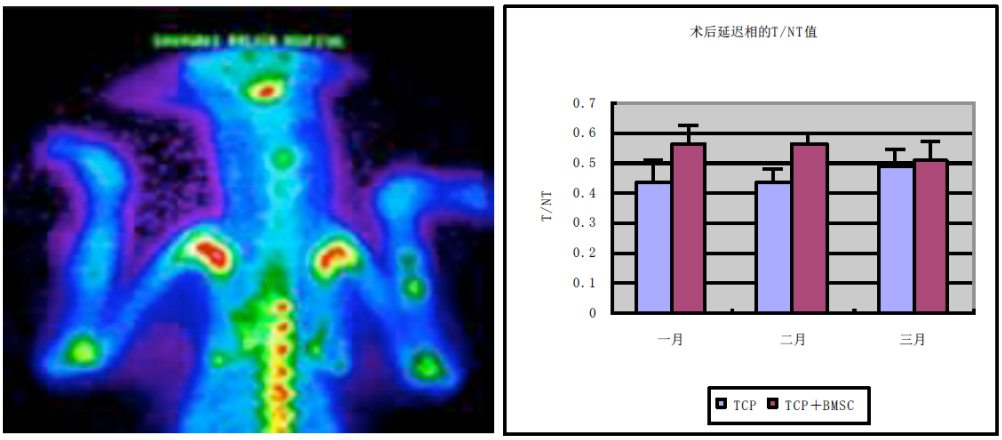

Figure 5: The phase delay bone imaging of each ulnar was taken by radionuclide scintigraph (left) and the T/NT rate was calculated at month one, two and three. there were significant difference (P< 0.65) between the two groups at month one and two, and there was no difference (P＝0.65)at month three By the Wilcoxon's signed rank test.

TCP degraded into fine granule with intrinsic porous network structure, and new bone adhered to the surface on the core of β-TCP in experimental group. In control group, HE staining showed that the degradation percentage was more than that of experimental group, osteoblasts orderly arranged on the surface of β-TCP holes, and osteoid was observed with much megacayocytes at the core of β-TCP in control group (Figure **4**). Moreover, in both groups, the interfaces were observed the similar histologic expression.

Radionuclide Scintigraphy

The phase delay bone imaging of each ulnar was taken by radionuclide scintigraph and the T/NT rate was calculated (Figure **5**) at month one, two and three. By the Wilcoxon's signed rank test, there were significant difference (P< 0.65) between the two groups at month one and two, and there was no difference (P = 0.65) at month three (Figure **5**).

DISCUSSION

Bone marrow stem cell (BMSC) is the most common-used seed cell in bone tissue engineering, due to its known osteogenic potential, scarcely invasive collection procedure and relatively simple culturing *in vitro* [16, 17]. Tough the novel polymeric and polymer-based composite scaffolds for bone tissue engineering have good structure and affinity [18-20], β-TCP which owns strong osteoconductivity and high biocompatibility has been attracting widely attention as a scaffold in bone regeneration. So in this study, TCP alone and TCP/BMSC constructs were chosen to evaluate the vascularization and osseointegration by scintigraphy, and the results of histological examination and radiography exactly showed that they were capable of forming bone *in vivo*.

Vascularization is an essential prerequisite for the engineered bone to survive and integrate with existing host tissue. After vascularized, the engineered bone can play an important role on bone formation through the production of growth factors, survival of various cells, transporting nutrition and eliminating the degradation products derived from the implant material. So the successful clinical graft derivate from tissue-engineered bone is dependent on the establishment of functional vascularization, and several strategies have been proposed and tested to accelerate the onset of neovascularization, such as seeding of mature and progenitor ECs, addition of angiogenic growth factors that elicit an angiogenic response *in vivo*, incorporation of microcapillary-like structures into the scaffold design that could provide the necessary physical cues for cells, and combining microsurgery techniques with tissue engineering concepts.

Different methods for assessing new-formed bone *in vivo* have been suggested, such as histological sections examination, radiography and CT. Those conventional methods depend on the two dimensional assessment of microvessel density without elaboration of the vascular. Hence, an adequate assay system should be found for the observation of angiogenic response to tissue-engineered bone *in vivo*.

Requirements for an ideal assay of quantitative angiogenesis have been described by Jain [21] as the following: (1) the structure and function of the new vasculature should be quantifiable; (2) newly formed vessels can be distinguished from pre-existing host

vessels; (3) tissue damage is avoided to prevent inflammation and its resulting neovascularization; (4) early noninvasive monitoring is possible; and (5) the system is economical, quick, simple, reproducible, and reliable. By comprehensive evaluation, bone scintigraphy meets some of the requirements, which has a high sensitivity and can demonstrate slight changes in bone [22]. Distribution of radiotracer can be shown and measured when accumulated and metabolized by relative tissue, that is, they provide information about the level of radiotracer activity [23].

Bone scintigraphy is a functional imaging technique with Tc-99m-MDP to track the bone metabolism activity [24]. The principle is that Tc-99m-MDP accumulates in areas of active bone turnover [25], depending on the degree of osteoblastic activity and vascularization [26, 27]. Bone scintigraphy can observe every type of osteoblastic activity, and it also enables the investigation of bone metabolism in per-implant zones [28]. This may provide important information related to the physiology and dynamic changes that occur during the osseointegration period [29].

The results of our study showed that bone scintigraphy may offer more information in the process of different periods and be clearer. Most importantly, it does not impact the animals and can be used *in vivo* for clinical usage, because this technology has often been used for diagnosis of carcinoma metastasis to provide informative diagnostic images [30, 31].

Obviously, bone scintigraphy is a good diagnostic tool in bone pathology. However, there are some disadvantages, such as bone scintigraphy show a pathological condition in less quantitation and resolution. The anatomical details are rather low [32].

CONCLUSION

This study may provide insight of bone scintigraphy into the clinical repair of long bone defect by tissue-engineered bone. Bone scintigraphy, although exhibiting less quantitation and resolution, would be applicable as a non-invasive, highly sensitive methodology in detecting the initial, microscopic changes associated with mineralization.

ACKNOWLEDGEMENTS

This study was supported by grants from the National Natural Scientific Foundation of China (81272019).

CONFLICT OF INTEREST

The authors have not disclosed any financial conflicts of interests.

REFERENCES

[1] Kasai T, Ishikawa K, Suzuki K, Yatani H. Initial evaluation of a ceramic form as reconstructive material for bone defect. Dent Mater J 2000; 19: 381-8. http://dx.doi.org/10.4012/dmj.19.381

[2] Nicholas RW, Lange TA. Granular tricalcium phosphate grafting of cavity lesions in human bone. Clin Orthop 1994; 306: 197-203.

[3] McAndrew MP, Gorman PW, Lange TA. Tricalcium phosphate as a bone graft substitute in trauma: Preliminary report. J Orthop Trauma 1988; 2: 333-9. http://dx.doi.org/10.1097/00005131-198802040-00011

[4] Vanassche BJ, Stoelinga PJ, de Koomen HA, Blijdorp PA, Schenaers JH. Reconstruction of the severely resorbed mandible with interposed bone grafts and hydroxyapatite: A 2-3 year follow-up. Int J Oral Maxillofac Surg 1988; 17: 157-60. http://dx.doi.org/10.1016/S0901-5027(88)80021-3

[5] Albrektsson T. Microangiographic representation of the microvascular system in bone tissue: a vital microscopic evaluation in the rabbit. Clin Orthop Relat Res 1981; (159): 286-93.

[6] Ren LL, Ma DY, Feng X, Mao TQ. A novel strategy for prefabrication of large andaxially vascularized tissue engineered bone by using an arteriovenous loop. Med Hypo 2008; 71: 737-40. http://dx.doi.org/10.1016/j.mehy.2008.06.032

[7] Marina IS. Vascularization in Bone Tissue Engineering: Physiology, Current Strategies, Major Hurdles and Future Challenges. Macromol Biosci 2010; 10: 12-27. http://dx.doi.org/10.1002/mabi.200900107

[8] Correia C, Grayson WL, Park M, *et al*. *In vitro* Model of Vascularized Bone: Synergizing Vascular Development and Osteogenesis. PLoS ONE 2011; 12: 6-12.

[9] Xin-Jun S, Wei P, Zai-Liang Y, Ming-Liang R. Heparin-Chitosan-Coated Acellular Bone Matrix Enhances Perfusion of Blood and Vascularization in Bone Tissue Engineering Scaffolds. Tissue Eng Part A 2011; 17(19-20): 2369-78. http://dx.doi.org/10.1089/ten.tea.2011.0027

[10] Brägger U. Digital imaging in periodontal radiography. A review. J Clin Periodontol 1988; 15(9): 551-7. http://dx.doi.org/10.1111/j.1600-051X.1988.tb02128.x

[11] Brägger U, Pasquali L, Kornman KS. Remodelling of interdental alveolar bone after periodontal flap procedures assessed by means of computer-assisted densitometric image analysis (CADIA). J Clin Periodontol 1988; 15(9): 558-64. http://dx.doi.org/10.1111/j.1600-051X.1988.tb02129.x

[12] Young S, Kretlow JD, Nguyen C, *et al*. Microcomputed Tomography Characterization of Neovascularization in Bone Tissue Engineering Applications. Tissue Eng Part B Rev 2008; 14(3): 295-306. http://dx.doi.org/10.1089/ten.teb.2008.0153

[13] Berding G, Bothe K, Gratz KF, Schmelzeisen R, Neukam FW, Hundeshagen H. Bone scintigraphy in the evaluation of bone grafts used for mandibular reconstruction. Eur J Nucl Med 1994; 21(2): 113-7. http://dx.doi.org/10.1007/BF00175757

[14] Stvrtecky RO, Kaufman M, Borgetti Z. Bone scintigraphy and osseointegration (preliminary report). J Oral Implantol 1995; 21(3): 239-42.

[15] Bambini F, Memè L, Procaccini M, Rossi B, Lo Muzio L. Bone scintigraphy and SPECT in the evaluation of the osseointegrative response to immediate prosthetic loading of endosseous implants: a pilot study. Int J Oral Maxillofac Implants 2004; 19(1): 80-6.

[16] Martin I, Muraglia A, Campanile G, Cancedda R, Quarto R. Fibroblast growth factor-2 supports *ex vivo* expansion and maintenance of osteogenic precursors from human bone marrow. Endocrinology 1997; 138(10): 4456-62.

[17] Muraglia A, Martin I, Cancedda R, Quarto R. A nude mouse model for human bone formation in unloaded conditions. Bone 1998; 22(5 Suppl): 131S-134S. http://dx.doi.org/10.1016/S8756-3282(98)00009-X

[18] Domingos M, *et al*. Improved osteoblast cell affinity on plasma-modified 3-D extruded PCL scaffolds. Acta Biomater 2013; 9(4): 5997-6005. http://dx.doi.org/10.1016/j.actbio.2012.12.031

[19] Puppi D, *et al*. Additive manufacturing of wet-spun polymeric scaffolds for bone tissue engineering. Biomed Microdevices 2012; 14(6): 1115-27. http://dx.doi.org/10.1007/s10544-012-9677-0

[20] Gloria A, Russo T, D'Amora U, *et al*. Magnetic poly(epsilon-caprolactone)/iron-doped hydroxyapatite nanocomposite substrates for advanced bone tissue engineering. J R Soc Interface 2013; 10(80): 20120833. http://dx.doi.org/10.1098/rsif.2012.0833

[21] Jain RK, Schlenger K, Hockel M, and Yuan F. Quantitative angiogenesis assays: progress and problems. Nat Med 1997; 3(11): 1203-8. http://dx.doi.org/10.1038/nm1197-1203

[22] Sklaroff DM, Charkes ND. Studies of metastatic bone lesions with strontium 85. Radiology 1963; 80: 270-2. http://dx.doi.org/10.1148/80.2.270

[23] Thomann KH, Dul MW. Bone scintigraphy: a review of the procedure and its applications. Optometry and Vision Science 1994; 71: 502-7. http://dx.doi.org/10.1097/00006324-199408000-00003

[24] Mari C, Catafau A, Carrio I. Bone scintigraphy and metabolic disorders. Quart J Nucl Med 1999; 43: 259-67

[25] Kanishi D. 99mTc-MDP accumulation mechanisms in bone. Oral Sur Oral Med and Oral Path 1993; 75: 239-46. http://dx.doi.org/10.1016/0030-4220(93)90100-I

[26] Schwartz Z, Shani J, Soskolne WA, Touma H, Amir D, Sela J. Uptake and biodistribution of technetium-99m-MD32P during rat tibial bone repair. J Nucl Med 1993; 34: 104-8. http://dx.doi.org/10.1034/j.1600-0501.2001.012004372.x

[27] McCracken M, Zinn K, Lemons JE, Thompson JA, Feldman D. Radioimaging of implants in rats using Tc-99m-MDP. Clinic Oral Implants Res 2001; 12: 372-8.

[28] Bambini F, Meme L, Procaccini M, Rossi B, Lo Muzio L. Bone scintigraphy and SPECT in the evaluation of the osseointegrative response to immediate prosthetic loading of endosseous implants: a pilot study. Inter J Oral Maxillofac Impl 2004; 19: 80-6.

[29] Cervelli V, Cipriani C, Migliano E, Giudiceandrea F, Cervelli G, Grimaldi M. SPECT in the long-term evaluation of osteointegration in intraoral and extraoral implantology. J Craniof Surg 1997; 8: 379-82. http://dx.doi.org/10.1097/00001665-199708050-00009

[30] Han CS, Wood MB, Bishop AT, Cooney WP. 3rd. Vascularized bone transfer. J Bone Joint Surg Am 1992; 74(10): 1441-9.

[31] McKiernan FE. Technetium-99m-methyl diphosphonate bone scintigraphy may be helpful in preoperative planning for vertebroplasty in multiple myeloma: two cases. J Vasc Interv Radiol 2010; 21(9): 1462-4. http://dx.doi.org/10.1016/j.jvir.2010.04.032

[32] Abdullah K, Ercan D, Güngör T, Kubilay I, Özgür I. Evaluation of osteoblastic activity around dental implants using bone scintigraphy. John Wiley 2010; 209-12.

Received on 06-11-2014 Accepted on 30-11-2014 Published on 19-12-2014

DOI: http://dx.doi.org/10.12970/2311-9888.2014.02.02.6